Automated setup for *ex vivo* larynx experiments

Veronika Birk,[1,a)] Michael Döllinger,[1] Alexander Sutor,[2] David A. Berry,[3] Dominik Gedeon,[2] Maximilian Traxdorf,[4] Olaf Wendler,[5] Christopher Bohr,[1] and Stefan Kniesburges[1]

[1]*Medical School, Division of Phoniatrics and Pediatric Audiology at the Department of Otorhinolaryngology Head and Neck Surgery, University Hospital Erlangen, Raumerstrasse 1a, 91054 Erlangen, Germany*

[2]*Chair of Sensor Technology, Friedrich-Alexander-University Erlangen-Nürnberg, Paul-Gordan-Strasse 3/5, 91052 Erlangen, Germany*

[3]*Laryngeal Dynamics Laboratory, Division of Head and Neck Surgery, David Geffen School of Medicine at UCLA, 10833 Le Conte Avenue, Los Angeles, California 90095-1624, USA*

[4]*Department of Otorhinolaryngology Head and Neck Surgery, University Hospital Erlangen, Waldstrasse 1, 91054 Erlangen, Germany*

[5]*Laboratory for Molecular Biology at the Department of Otorhinolaryngology Head and Neck Surgery, University Hospital Erlangen, Waldstrasse 1, 91054 Erlangen, Germany*

(Received 14 September 2016; revised 9 January 2017; accepted 12 January 2017; published online 2 March 2017)

Ex vivo larynx experiments are limited in time due to degeneration of the laryngeal tissues. In order to acquire a significant and comparable amount of data, automatization of current manual experimental procedures is desirable. A computer controlled, electro-mechanical setup was developed for time-dependent variation of specific physiological parameters, including adduction and elongation level of the vocal folds and glottal flow. The setup offers a standardized method to induce defined forces on the laryngeal cartilages. Furthermore, phonation onset is detected automatically and the subsequent measurement procedure is automated and standardized to improve the efficiency of the experimental process. The setup was validated using four *ex vivo* porcine larynges, whereas each validation measurement series was executed with one separate larynx. Altogether 31 single measurements were undertaken, which can be summed up to a total experimental time of about 4 min. Vocal fold elongation and adduction lead both to an increase in fundamental frequency and subglottal pressure. Measurement procedures like applying defined subglottal pressure steps and onset-offset detection were reliably executed. The setup allows for a computer-based parameter control, which enables fast experimental execution over a wide range of laryngeal configurations. This maximizes the number of measurements and reduces personal effort compared with manual procedures.
© *2017 Acoustical Society of America*. [http://dx.doi.org/10.1121/1.4976085]

[JFL] Pages: 1349–1359

I. INTRODUCTION

Voice results from periodic oscillation of the vocal folds in the larynx. The oscillation is caused by a fluid-structure interaction between the tracheal flow from the lungs and the elastic tissue of the vocal folds. This oscillation produces the primary sound signal, which is subsequently modulated by the vocal tract. Pre-phonatory vocal fold posture (vocal fold adduction and elongation) has a significant influence on the amplitude and frequency of oscillation of the vocal folds and on the loudness of the resulting acoustic signal.[1]

Figure 1 depicts a schematic of the top view of the larynx with an open glottis (top left) for breathing and with a closed glottis (top right) for initiation of the phonatory process. *In vivo*, the cartilages perform a complex three-dimensional maneuver to transform the larynx from a respiratory to a phonatory posture.[2] Vocal fold adduction is achieved by a complex interaction of three intrinsic muscles resulting in a rotation, translation, and tilting of the arytenoid cartilages.[2]

Lengthening and narrowing of the vocal folds is produced by a contraction of the cricothyroid muscle. The resulting motion of the thyroid cartilage is an anteroposterior sliding motion and rotation in the cricothyroid joint;[3] see Fig. 1, bottom.

In vivo, glottal parameters like muscle tension or glottal airflow are not directly measurable and cannot be controlled independently from each other. Therefore, *in vivo* and *ex vivo* models are used for detailed investigation of the influence of parameter variation (e.g., vocal fold adduction and elongation) on the phonatory process. Chhetri *et al.*[4] used *in vivo* canine larynx models in which the intrinsic laryngeal muscles were activated through graded stimulation. This is a sophisticated procedure, requiring profound surgical skill to expose individual branches of the laryngeal nerves.

Ex vivo larynx experiments present an alternative to *in vivo* experiments.[5–12] With the *ex vivo* model, it is a big challenge to simulate the three-dimensional motions of the cartilages caused by a complex interplay of muscle contraction *in vivo*. Therefore, these experiments are based on simplified cartilage motions like an axial rotation or one-dimensional translational motion.[11,13,14]

Static and manual control of the cartilage position in *ex vivo* larynges is often achieved by mechanical devices like sutures or screws.[15] For simulation of the cricothyroid

[a)]Electronic mail address: veronika.birk@uk-erlangen.de

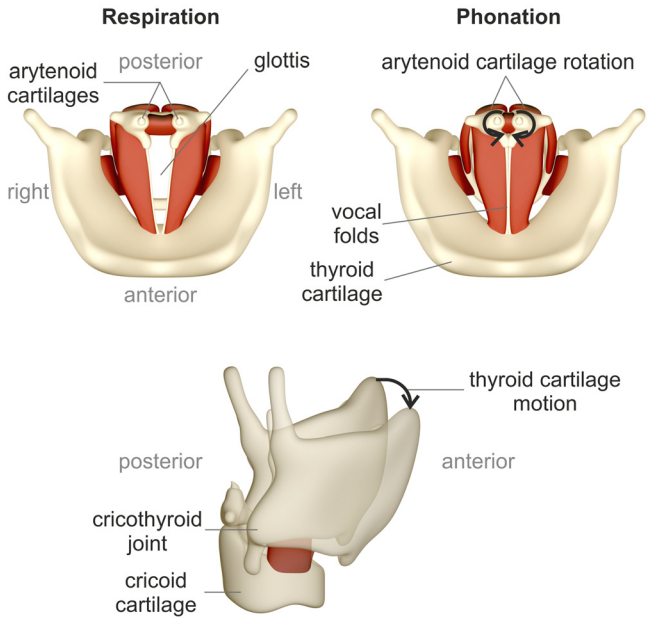

FIG. 1. (Color online) Top and lateral view of the larynx, based on Luegmair (Ref. 17). (Top left) Open glottis for breathing, (top right) phonation posture with closed glottis. (Bottom) Thyroid cartilage motion including an anteroposterior sliding and tilting.

muscle contraction, a force is applied on the thyroid cartilage, e.g., by sutures.[16] Adduction of the vocal folds can be achieved by simulating the lateral cricoarytenoid muscle contraction, which internally rotates the arytenoid cartilages.[3] By applying a force to the lateral part of the arytenoid cartilage in anterior direction, e.g., by a weight, the arytenoid cartilage rotates internally and closes the glottis.[13,14]

Both symmetric as well as asymmetric vocal fold posture can be simulated by these experiments.[13,16,18–20]

This offers the possibility to simulate voice disorders that are related to an abnormal vocal fold posturing during phonation caused by excessive or poorly regulated muscle activity, called muscle tension dysphonia.[3]

The elaborate preparation of the larynx and the manual procedure of parameter variation during the experiments is very time consuming. However, time is a very critical factor in executing *ex vivo* larynx experiments due to tissue dehydration causing changes in the oscillation behavior of the vocal folds.[21] Therefore, an optimization of the experimental procedure is desirable.

Phonation is initiated and driven by an airstream from the lungs. The subglottal pressure P_S required for initiating and sustaining the phonatory process was defined by Titze[1] as phonation threshold pressure *ptp*. Several studies show the clinical significance of *ptp* whereas its assessment can be either direct or indirect.[22] A direct measurement of P_S *in vivo* is either invasive or intrusive and very time consuming.[22] *Ex vivo* larynx experiments offer the opportunity to directly measure P_S by a pressure sensor applied directly below the vocal folds. In these experiments the glottal airflow is gradually increased until vocal fold oscillation occurs.

For a fast experimental execution, an effective onset detection during the experiment is desirable. Phonation onset detection can be executed by subjective[10,12,23–33] or objective[9,34–38] methods determining the characteristics of the high-speed video, P_S, acoustic, or electroglottographic signals.

Many studies include an objective method that is based on the video signal.[36–38] Due to the high processing time for video data this procedure is not suitable for onset detection in real time. Jiang *et al.*[9] use the root mean square of the acoustic signal, which enables a fast and objective onset detection. Nevertheless, this procedure is based on a signal that includes a high noise component, depending on the experimental conditions, which poses the risk of errors caused by background noise. Mau *et al.*[33] determined the onset on the basis of the relative amplitude and periodicity of the subglottal pressure signal after the measurement. Due to its low noise component and the possibility of high-speed sampling and processing, we assess P_S as a suitable signal for real-time onset detection.

In most studies, glottal airflow is physically controlled, whereas from a physiological point of view, the subglottal pressure is the essential variable. Therefore, a direct glottal flow control on the basis of the subglottal pressure signal is desirable. This offers the opportunity to adjust defined subglottal pressure values to the system.

Variability of measurement results can be referred to several factors:

(1) Anatomical variations between each larynx.
(2) Individual larynx preparation.
(3) Individual fixation of the larynx in the experimental setup.
(4) Degeneration of the larynx tissue due to extensive experimental time.
(5) Manual variation of parameters like vocal fold adduction by weights.

The first three items cannot be influenced. The aim of this study is to minimize the experimental procedure duration and to facilitate the variation of parameters in *ex vivo* larynx experiments to minimize the influence of items 4 and 5 on the variability of experimental results. This includes a computer controlled variation of parameters, including vocal fold adduction and elongation, by electro-mechanical devices. Furthermore, the tracheal airflow is controlled on the basis of P_S as feedback parameter. This offers the possibility of an automated onset detection.

To gain a deeper insight regarding voice production, a maximum number of experimental conditions have to be implemented with one single excised larynx in the shortest time possible using a standardized experimental procedure. Hence, an automatization is essential for acquiring sufficient experimental data and for minimizing dehydration of *ex vivo* larynges during the experimentation.

II. EXPERIMENTAL SETUP

In order to minimize the experimental procedure duration and to facilitate the variation of parameters, a customized, computer controlled setup was developed. Specifically, a time-dependent variation of vocal fold adduction, vocal

fold elongation, and P_S is achieved by controlling the following parameters:

(1) Rotation of the arytenoid cartilages.
(2) A tilt of the thyroid cartilage.
(3) Laryngeal airflow.

Figure 2 shows the experimental setup, including the customized electro-mechanical devices for cartilage posturing and mounting of the larynx. The individual modules and the data acquisition devices are explained in the following.

The *ex vivo* larynx is mounted on an artificial tracheal tube of stainless steel with a diameter of 20 mm, dimensioned for porcine larynges, including a hole drilled for a subglottal pressure sensor 130 mm below the glottis. A custom-made support prevents a lateral displacement of the larynx. It consists of a tube made from polyvinyl chloride (PVC) and screws fixing the cricoid cartilage. An opening in the tube at the ventral side allows for a tilt of the thyroid cartilage; see Fig. 2.

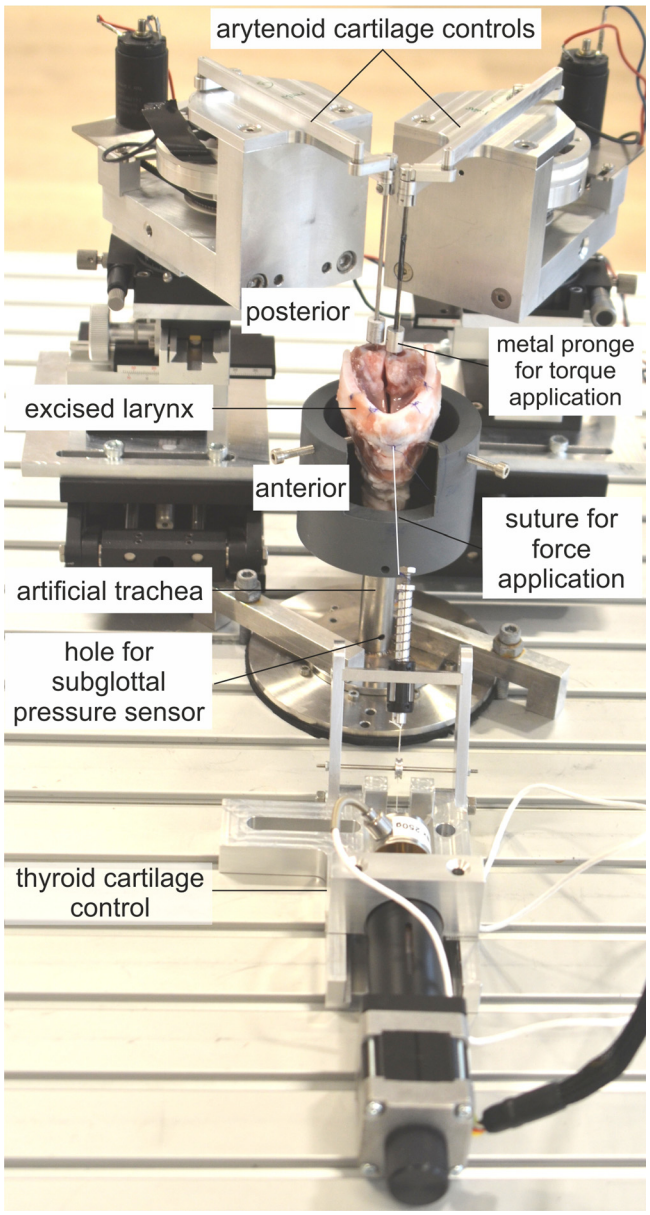

FIG. 2. (Color online) Experimental setup for thyroid and arytenoid cartilage motion. Vocal fold elongation is achieved by applying a force to the thyroid cartilage leading to a tilt. Inducing a torque in the arytenoid cartilages leads to a rotation and creates vocal fold adduction.

The subglottal pressure is captured by a XCS-93-5PSISG (Kulite Semi-Conductor GmbH, Kaiserslautern, Germany) pressure sensor, which is flush-mounted to the internal wall of the artificial trachea. The pressure sensor is driven by a PXIe-4330 (National Instruments, Austin, TX) bridge module offering a 24 bit resolution. The acoustic pressure signal Pa is captured by a 4189 [Brüel & Kjær Sound & Vibration Measurement A/S (Hq), Nærum, Denmark] 1/2-inch free-field microphone mounted in coronal plane of the larynx with a 45° inclination toward the sagittal plane at a distance of 30 cm to the glottis. The microphone is driven by a Nexus 2690 microphone conditioning amplifier (Brüel and Kjaer). The amplified signal is captured by a 4492 (National Instruments) dynamic signal acquisition module with a 24 bit resolution.

The vocal fold motion is recorded by a Phantom V2511 (Vision Research, Wayne, NJ) high-speed camera with an EF 180 mm f/3.5 macro lens (Canon, Inc., Tokyo, Japan). To synchronize the high-speed recordings with the acoustic and subglottal pressure signals, the camera state signals are captured by a 6356 (National Instruments) multifunctional data acquisition module with a 16 bit resolution. This module is also used to send a start trigger to the camera to initiate the recording.

The three mentioned National Instruments modules are integrated in a PXIe-1073 (National Instruments) express chassis allowing for a synchronization of the captured data. The whole setup is controlled by a PC via LabVIEW (National Instruments). The front panel of the controlling program is depicted in Fig. 3 and shows the different input and output boxes of the controlling interface.

A. Thyroid cartilage control

To simulate cricothyroid muscle contraction, a customized electro-mechanical setup was built, which applies a defined force to the thyroid cartilage leading to a tilting of the cartilage as shown in Fig. 1. This approach is equivalent to the control by weights as reported in the literature,[16,41] but has the advantage that it enables an electro-mechanical control of this parameter. The cricothyroid joint serves as a natural hinge for the rotation process. The electro-mechanical setup, depicted in Fig. 4, top, consists of an applicator that is fixed with a surgical suture on the tip of the thyroid cartilage. Moving the linear stepper motor M-229.26 S [Physik Instrumente (PI) GmbH & Co. KG, Karlsruhe, Germany], the force (depicted with arrows) is redirected from the horizontal plane toward the tip of the thyroid cartilage by a low-friction ball bearing.

The thyroid force is measured by a 31 E-2N5-1 a (Althen GmbH Meß- und Sensortechnik, Kelkheim, Germany) force sensor, which consists of a piezo resistive strain gauge connected in a full bridge configuration. The measurement range of the sensor lies within 0 N and 2.5 N with an accuracy of ±0.15%. It is operated using a PXIe-4331 (National Instruments) dynamic bridge module. The sensor range was chosen on basis of the investigation of Vilkman[11] who used a maximum force of 1.5 N for the elongation of the vocal folds in an *ex vivo* human larynx model.

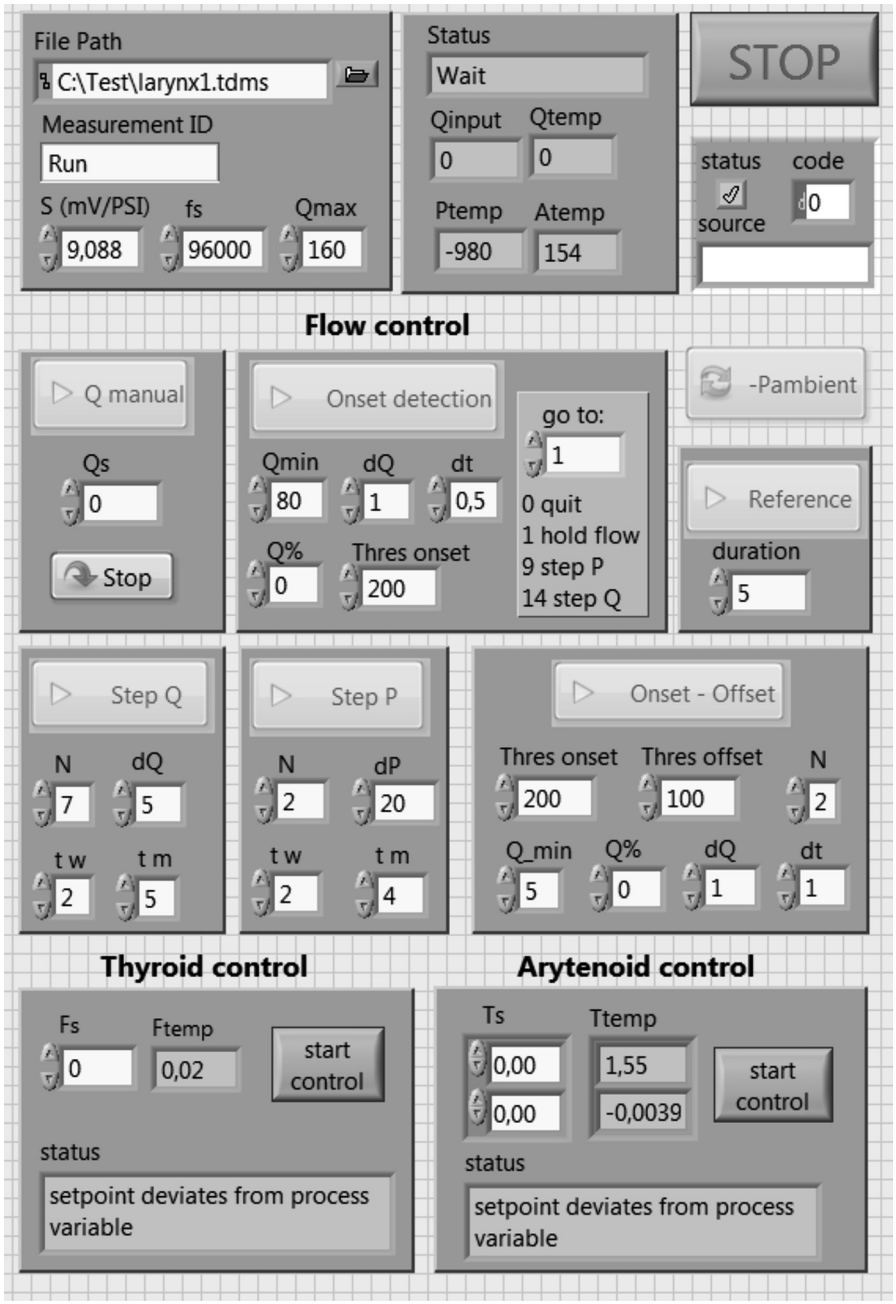

FIG. 3. Front panel of the controlling software implemented in LabVIEW. The interface includes input and output boxes for the flow and cartilage control.

The force serves as feedback control parameter for the controlling circuit realized in LabVIEW. The actuating variable, namely, the travel distance of the motor, is transferred to the motor controller C-663 (Physik Instrumente) via a universal serial bus port (USB), which enables a minimum step size of 1 μm.

The lower picture in Fig. 4 shows a top view of the larynx before and after the application of a force on the thyroid cartilage. The arrow in Fig. 4(a) shows the direction of the force, which was increased from 0 N to 2 N. The resulting vocal fold elongation is depicted in Fig. 4(b). The arrows indicate vocal fold length before and after the force application.

B. Arytenoid cartilage control

Vocal fold adduction can be achieved by a rotation of the arytenoid cartilages as depicted in Fig. 1, top. For a torque controlled rotation of the arytenoid cartilages, two devices were developed and constructed, as depicted in Fig. 5, top.

The applicator, consisting of a prong with three needles, is pricked to the upper part of the arytenoid cartilage. By rotation of the applicator, the torque is directly applied to the cartilages.

The rotation is produced by a 2626 024 CR (Dr. Fritz Faulhaber GmbH & Co. KG, Schönaich, Germany) DC-motor and redirected over a kinematic chain to the applicators. The applied torque is measured using a TD70 (ME Meßsysteme GmbH, Hennigsdorf, Germany) torque sensor, which is driven by a customized bridge module. The resulting feedback control parameter is processed by a proportional, integral, and differential (PID) controller implemented in LabVIEW. The actuating variable is transferred to the current amplifier, which drives the motor. The setup allows for a maximum torque application of 25 mNm

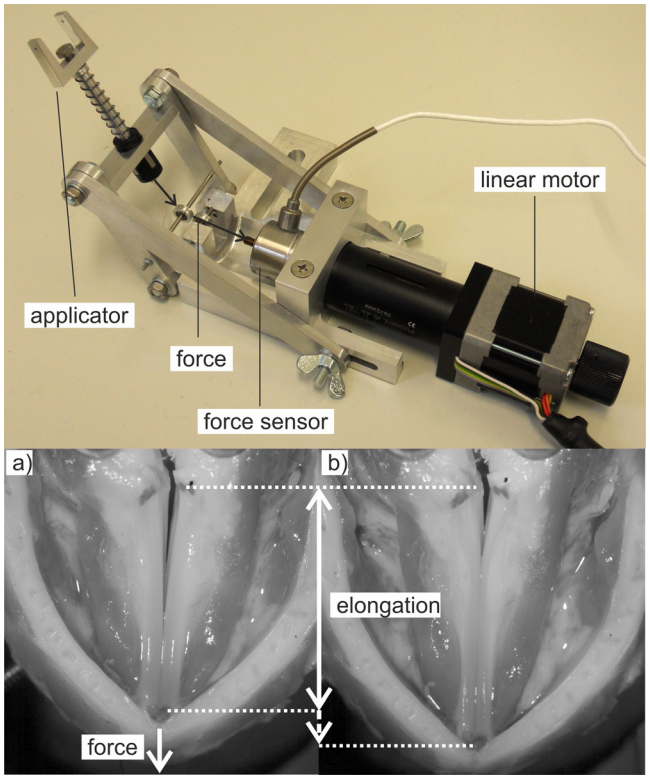

FIG. 4. (Color online) (Top) Electro-mechanical setup for applying a force to the thyroid cartilage. (Bottom) (a) the arrow depicts the force applied to the cartilage, (b) vocal folds are elongated compared with the vocal folds in (a).

with a minimum step size of 0.1 mNm and a maximum rotation angle of 90°. The setup was designed based on the examinations of axial rotation angle of Kasperbauer[39] and *ex vivo* examinations that used sutures and weights to achieve

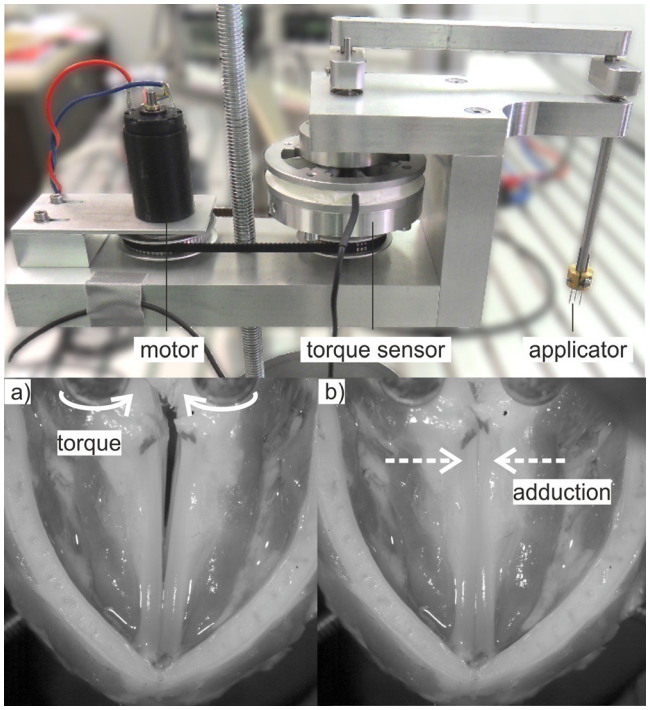

FIG. 5. (Color online) (Top) Electro-mechanical setup for arytenoid cartilage rotation. (Bottom) The arrows in (a) depict the torque applied to the arytenoid cartilages. (b) shows the resulting vocal fold adduction.

axial rotation.[7,14,41] Other parameters (thyroid force and glottal flow) were chosen to gain a stable phonation with medium vocal fold elongation. Glottal flow steps of 5 slm (standard liters per minute) have proven to induce distinct changes in the vocal fold dynamic in previous experiments with *ex vivo* porcine larynges.

The applied asymmetry A is calculated from the imbalance between the induced torques DR/L in the right and the left arytenoid cartilage:[40]

$$A = \frac{D_R - D_L}{D_R + D_L} \times 100\%. \quad (1)$$

In the following, the adjusted asymmetry is zero to examine the influence of the vocal fold adduction level.

The resulting vocal fold adduction is depicted in Fig. 5, bottom with an applied torque of 0 mNm [Fig. 5(a)] and 25 mNm [Fig. 5(b)]. The arrows in Fig. 5(a) indicate the torque applied to the arytenoid cartilages; the arrows in Fig. 5(b) show the resulting vocal fold adduction.

C. Laryngeal flow control

Glottal airflow is controlled via a RS232 interface by a 4000B digital power supply (MKS, Andover, MA) driving a 1579A/B (MKS) mass flow controller with an accuracy of ±2 slm.

The airflow is heated and humidified by an Ultrasonat 810 (Hico, Hirtz & Co. KG, Köln, Germany) ultrasound nebulizer preventing tissue dehydration. The air passes through a settling chamber (see Ref. 41), built in cooperation with the "Institute of Process Machinery and Systems Engineering, Friedrich-Alexander Universität Erlangen-Nürnberg," to dampen turbulent fluctuations in the inflow.

The laryngeal flow control is subdivided into two steps, as shown in Fig. 6:

(1) Onset detection (manual or automatic).
(2) Measurement function (flow steps, pressure steps, flow ramp).

The onset can be detected manually by increasing the flow stepwise via the user interface and evaluating the sound signal subjectively.

The automated onset detection is based on the subglottal pressure signal P_S. This signal was found to be suitable for an onset detection in real time because it contains less noise than the acoustic output signal and can be processed considerably faster than the video signal.

The integrated algorithm uses the peak-to-peak amplitude of P_S. If the amplitude exceeds/drops below a specific threshold, determined by the operator, the onset/offset is being detected.

For the automated measurement functions "flow steps" and "pressure steps," the flow rate is further increased by a specified percentage of the onset flow-rate to help ensure stable phonatory conditions.

For the measurement function flow steps, the flow is directly transferred to the mass flow controller. The step size and measurement duration is pre-defined by the operator.

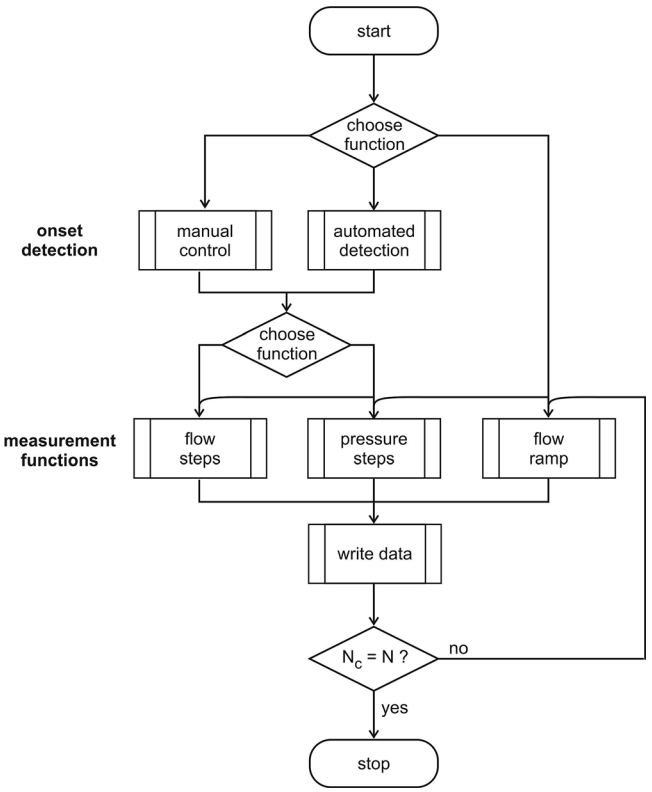

FIG. 6. Flow chart of the laryngeal flow control including manual and automatic onset detection and the measurement functions "flow steps," "pressure steps," and "flow ramp."

For the pressure steps measurement, the pressure steps, selected by the operator, are adjusted by a PID controller implemented in LabVIEW controlling the mass flow on the basis of the average subglottal pressure signal $\bar{P}_S$.

Data acquisition is started after a pre-defined waiting time t_w. This ensures a stabilization of the system. In the flow steps procedure, glottal flow is kept constant and the measurement is started after t_w has expired. In the pressure step procedure, stable oscillation conditions are reached when the mean subglottal pressure ranges within an interval of ± 20 Pa around the selected subglottal pressure for a time interval of t_w. This is realized by a PID controller that adjusts the flow rate on the basis of the subglottal pressure signal. After t_w has expired, subsequently, the measurement period is started and the data are recorded at constant flow rate conditions.

The measurement function "flow ramp" operates without initial onset detection and passes through N cycles of onset and offset that are detected automatically. This procedure serves for the analysis of *ptp* and offset pressure, which are determined in a post-processing step after the measurement and offers the possibility to investigate the variance of the individual onset and offset pressure values.

The complete control circuit allows for a parameter adjustment with a control loop time of 200 ms.

D. Larynx preparation

Porcine cadaver larynges were used to validate the experimental setup. The larynges were quick frozen with 2-Methylbutan (–150 °C) and stored at −80 °C in order to preserve the tissue properties until the experiment.[42] The larynges were slowly thawed in a refrigerator and kept wet using NaCl solution 12 h before the experiment.

Subsequently, the larynges were prepared for the experiments by removing supraglottal structures to the level of the ventricular folds. The upper part of the arytenoid cartilages was removed to generate a contact area for the arytenoid manipulator prongs.

A suture was fixed to the tip of the thyroid cartilage to mount the thyroid control setup. For each of the following validation measurements one separate larynx was used to demonstrate the functionality of the setup. Altogether four larynges were used in this work.

III. VALIDATION OF EXPERIMENTAL SETUP

The following test measurements demonstrate the functionality of the computer controlled setup. For data acquisition, the following parameters were selected. Acoustic and subglottal pressure signals were captured with a sampling rate of 50 kHz and duration of 5 s. The high-speed video was recorded with a frame rate of 4000 fps, a spatial resolution of 768 px × 768 px, and a duration of 0.6 s. The following measurements show the influence of vocal fold elongation and adduction on the phonatory process. The automated onset detection is demonstrated by a cyclic onset-offset measurement executed by the "ramp function." The pressure steps measurement demonstrates the execution of the measurement functions.

Aerodynamic parameters were calculated and compared to similar *ex vivo* larynx experiments in literature. This paper contains multimedia material, provided by the authors. This includes three avi format movie clips (Mm. 1–Mm. 3), which show the high-speed video re-sampled to 25 fps of the excised larynges during the three test scenarios. The corresponding audio signal is also provided (Mm. 4).

A. Vocal fold elongation

The force applied to the thyroid cartilage F, elongating the vocal folds, was varied between 0.5 N and 2 N with a step size of 0.5 N. This represents the range between a minimal vocal fold elongation, required for phonation and an extreme vocal fold elongation. This range was chosen on basis of Vilkman[11] who used a maximum force of 1.5 N for thyroid cartilage rotation. The glottal flow Q was kept constant at 30 slm, which was a medium flow value that guaranteed a stable phonation. The induced arytenoid torque T in both cartilages was kept constant at 10 mNm, which represents a medium vocal fold adduction according to the literature.[7,14,41]

Figure 7 depicts $\bar{P}_S$ (solid line) and fundamental frequency f_0 (dashed line) for different thyroid force steps. $\bar{P}_S$ increases with increasing vocal fold elongation resulted from increased thyroid force. This was described by Alipour *et al.*[43] who investigated the influence of vocal fold elongation on *ex vivo* canine larynges using a force applied by a suture.

The fundamental frequency also increased with increasing thyroid force. This phenomenon is also described in Chhetri *et al.*[44] and Hsiao *et al.*[45] who investigated vocal

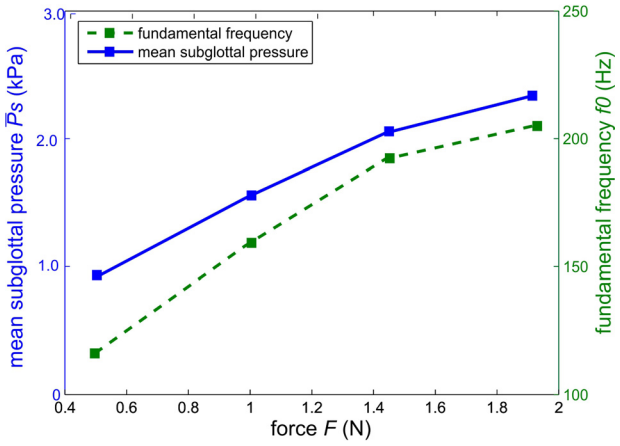

FIG. 7. (Color online) Mean subglottal pressure and fundamental frequency as a function of the force applied to the thyroid cartilage.

fold elongation as a function of cricothyroid muscle activation in canine larynges. Alipour *et al.*[5] also reported an increase in f_0 using sutures for vocal fold elongation in canine larynges. Furthermore, Vilkman[11] reported an increase in $\bar{P}_S$ and f_0 as a function of vocal fold elongation, achieved by thyroid cartilage rotation, in *ex vivo* human larynges.

Mm. 1. The video shows the *ex vivo* larynx during phonation while the thyroid force is being increased stepwise. The fundamental frequency increases with elongation of the vocal folds, as perceivable in the audio signal. This is a file of type "avi" (1.4 Mb).

B. Vocal fold adduction

The torque induced in both arytenoid cartilages, adducting the vocal folds, was varied from 5 mNm to 25 mNm with a step size of 10 mNm, Q was increased stepwise ($\Delta Q = 5$ slm) and F was kept constant at 1 N.

Figure 8(top) depicts $\bar{P}_S$ as a function of the glottal flow for three arytenoid adduction levels, namely, 5, 15, and 25 mNm.

For increasing adduction level, a lower flow rate has to be applied to obtain the same subglottal pressure value. This was also shown in Alipour and Jaiswal[6] who investigated the influence of vocal fold adduction in porcine larynges. Hence, the trans-laryngeal flow resistance defined by van den Berg[46] increased with increasing arytenoid adduction, which was also shown by Döllinger *et al.*[47] who investigated the influence of the adduction level in human hemi-larynx experiments.

Figure 8 (bottom) shows f_0 as a function of mean subglottal pressure for three different adduction levels. Fundamental frequency increased for increasing subglottal pressure level. This was explained in Titze[48] who described this phenomenon as a result of the tension of the vocal folds being dependent on the oscillation amplitude. For increasing adduction level, the fundamental frequency increased for equal subglottal pressure levels. Increase in f_0 was also found

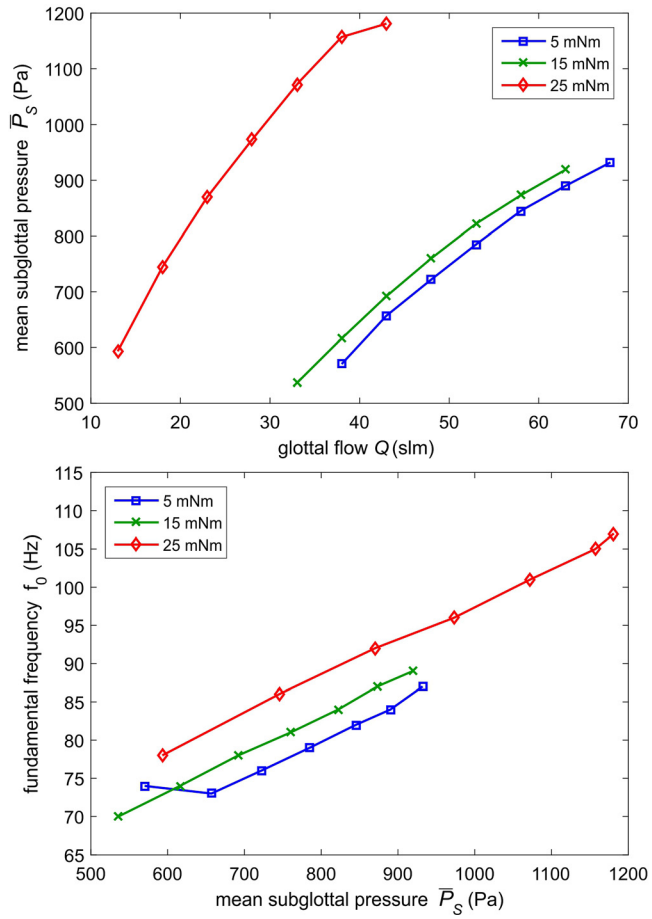

FIG. 8. (Color online) (Top) Mean subglottal pressure as a function of the glottal flow for different arytenoid adduction levels. (Bottom) Fundamental frequency as a function of the mean subglottal pressure for different arytenoid adduction levels.

in Alipour[7] who investigated the influence of vocal fold adduction on the phonatory process in porcine larynges.

Mm. 2. The video shows the *ex vivo* larynx during phonation at a constant flow of $Q = 40$ slm and different arytenoid adduction levels. The fundamental frequency increases, which can be perceived in the related audio signal. This is a file of type "avi" (1.0 Mb).

C. Pressure steps measurement

For the measurements, the torque was set to 10 mNm and the thyroid force was adjusted to 1 N. These medium values were chosen to gain a physiological phonation posture according to the literature.[7,11,14,41] After onset detection, the measurement function adjusts defined pressure steps, which were set to 200 Pa. This step size corresponds to a flow rate step of 5 slm at medium vocal fold elongation and adduction levels. The flow is controlled until $\bar{P}_S$ ranges in an interval of ± 20 Pa around the selected pressure for $t_w = 2$ s. These values have proven to be suitable to enable a measurement with pressure steps. Subsequently, the measurement is executed and the signals are captured for 4 s. The time dependent signals for two pressure steps are depicted in Fig. 9.

The first picture shows P_S and $\bar{P}_S$, and the second figure depicts the corresponding flow signal. The transition from step 1 to step 2 is not depicted in Fig. 9, solely the measurement signals at constant subglottal pressure levels are shown. The mean subglottal pressure in step 1 is $\bar{P}_S(\text{step1}) = 1571.2$ Pa, in step 2 $\bar{P}_S(\text{step2}) = 1778.0$ Pa. The mean pressure deviates from its set point [$\bar{P}_S(\text{step1}) + 200$ Pa] of 8.3 Pa. This deviation can be attributed to the accuracy of the flow controller (± 2 slm), which obstructs a more precise parameter control.

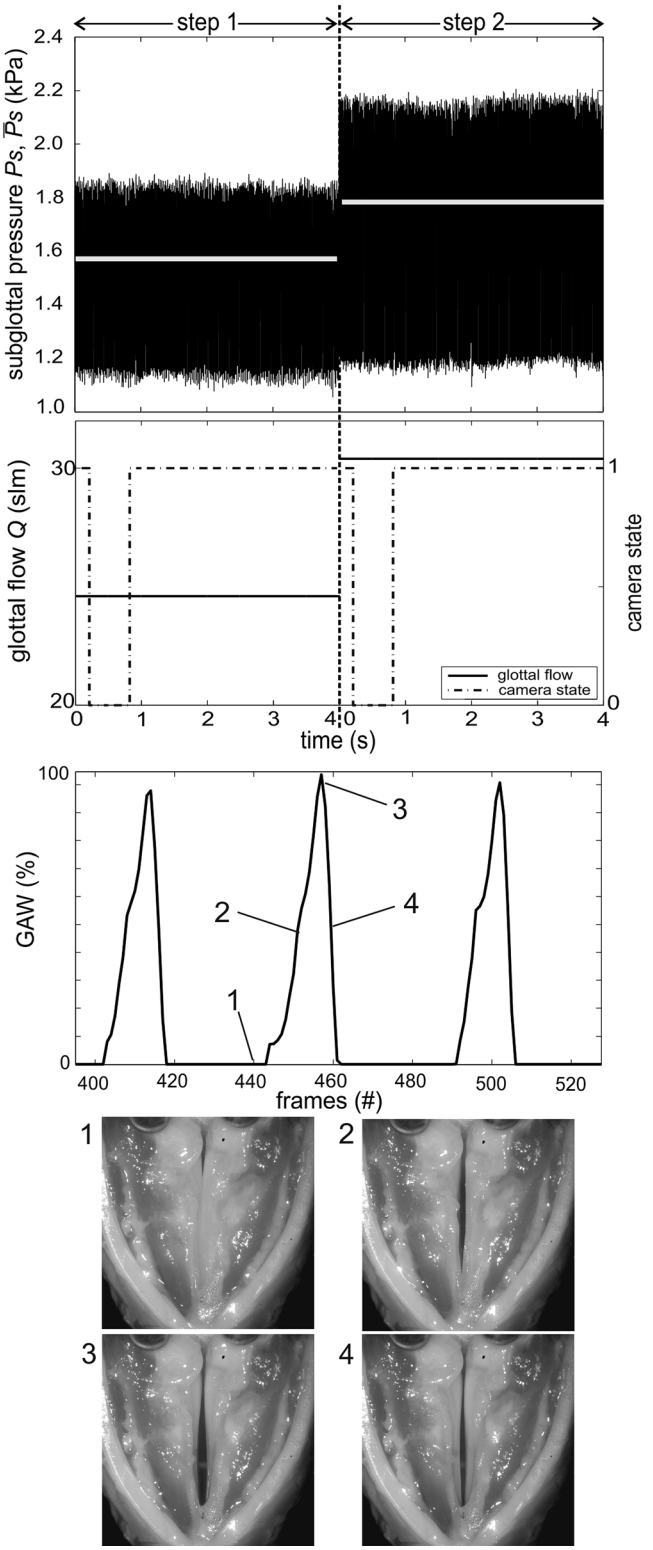

FIG. 9. Time resolved signals of the pressure steps measurement displaying the measuring time windows at the two pressure levels. Signals from top to bottom: mean and time resolved subglottal pressure, laryngeal flow, and camera state signal (low, recording; high, waiting for next trigger), GAW of step 1, picture of the larynx in the closed (1), opening (2), opened (3), and closing (4) phase. All signals are synchronized.

The camera state signal, depicted in the second figure, was used to synchronize the video recordings with the signals mentioned above. If the camera state signal is low, the camera is in the record mode; when the signal is high, the camera is waiting for the next trigger. The third picture shows three cycles of the glottal area waveform GAW calculated from the high speed video of step 1.[49] The GAW was computed using the in-house software tool Glottis Analysis Tools (GAT). The bottom pictures show the larynx in the closed (1), opening (2), opened (3), and closing (4) phases of one vibrational cycle.

D. Onset offset measurement

For the automated onset and offset measurement, which is executed using the flow ramp measurement function, the arytenoid torque ($T = 10$ mNm) and the thyroid force ($F = 1$ N) were constant for a phonation posture of the larynx. According to the pressure steps measurement, the elongation and adduction levels were chosen in medium levels according to the literature.[7,11,14,41] The minimum glottal flow was determined by manual flow increase until onset occurs. The starting value of flow rate was the set to $Q = 7$ slm, which was just below the offset flow to avoid long onset detection time. The flow rate step size was chosen to 0.2 slm per 0.2 s, to gain an optimal high-speed visualization of the onset process. Minimum glottal flow was set and the flow was sequentially increased, until the onset was detected. The flow was further increased to 110% of the onset flow threshold to ensure stable phonation. Subsequently, the flow was decreased until offset was detected and further decreased to 90% of offset flow threshold to ensure ceasing of the vocal fold vibration. This procedure was repeated several times. Hereby the transition from cessation to a stable phonation and vice versa can be investigated.

One onset and offset cycle is depicted in Fig. 10. The upper figure shows the time-resolved subglottal pressure signal. The onset and offset process is shown enlarged and depicts the transition from a non-oscillating to oscillating condition. The vertical lines represent the time points of onset and offset. The amplitude of the subglottal pressure increases from 90 Pa to 330 Pa at the onset and reverts to 90 Pa at the offset. The lower figure depicts $\bar{P}_S$ (solid line) and Q (dashed line) as a function of time. The mean subglottal pressure [$\bar{P}_S(\text{offset}) = 840$ Pa] and glottal flow [$Q(\text{offset}) = 9.6$ slm] at the offset is less than the onset pressure [$\bar{P}_S(\text{onset}) = 1325$ Pa] and flow [$Q(\text{onset}) = 13.4$ slm]; see Fig. 10 (bottom). This hysteresis effect has been reported elsewhere.[10,33]

Mm. 3. The video shows the onset process. This is a file of type "avi" (1.5 Mb).

Mm. 4. The related audio signal depicts the onset process. This is a file of type "wav" (2.5 Mb).

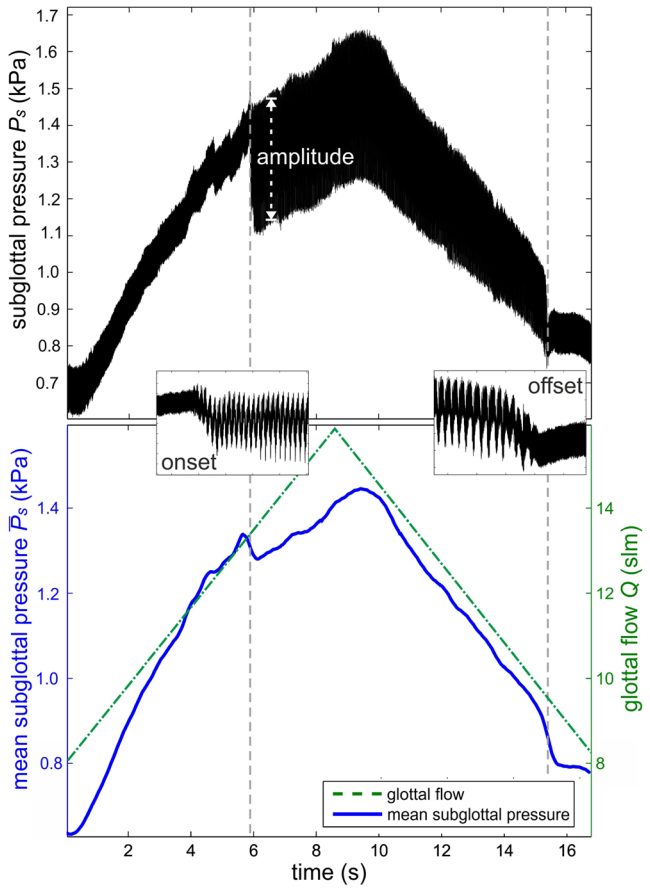

FIG. 10. (Color online) (Top) Time resolved subglottal pressure signal at sequentially increasing/decreasing glottal flow. (Bottom) Mean subglottal pressure signal (solid line) and glottal flow (dashed line) as a function of time. The first vertical line depicts the time point of onset, the second line the time point of offset detection.

IV. CONCLUSION

The customized setup offers computer controlled variation of pre-phonatory parameters, including vocal fold adduction and elongation, by electro-mechanical devices. Note that the complex three-dimensional cartilage motion is simplified to an arytenoid rotation, which simulates lateral cricoarytenoid muscle contraction.

Furthermore, the setup controls glottal airflow through means of the subglottal pressure. It includes an automated onset detection and several automated measurement functions.

The setup was validated using *ex vivo* porcine larynges. Different laryngeal adduction levels as well as vocal fold elongation adjustments were executed. Automated onset detection was demonstrated in onset-offset measurements. The results were compared to previous studies reporting aerodynamic investigations using manual parameter variation.

This combination of thyroid force, arytenoid torque, and glottal airflow control enables a fast experimental execution over a wide range of laryngeal configurations. This significantly reduces the experimental execution time, in comparison with manual experimental methods. Witt *et al.*[50] reported ∼10 min of experimental time after which the larynx was not able to phonate. The preliminary measurement series include seven force steps, seven flow steps with three adduction levels, two pressure steps, with a measurement duration of 5 s, respectively, and one onset-offset cycle. Together 31 single measurements were implemented using the present setup within a time span of about 4 min.

Due to the simplified fixation of the arytenoid cartilages by the electro-mechanic devices, a time-consuming laryngeal preparation including suture positioning[13,14] was avoided.

The automated onset detection which was based on the peak-to-peak amplitude of the subglottal pressure signal offered an objective onset detection in real time. This may be helpful in larger studies because of the high inter-subject variability with respect to phonation onset pressure.[33] Furthermore, the presented functionality makes an additional experimenter, stationed near the larynx for parameter variation, unnecessary. This may be beneficial in audio measurements in which the larynx is located in very quiet environments like an anechoic chamber.

Using control loop feedback mechanisms implemented in LabVIEW, the setup allows very small force/torque steps to be induced on the cartilages, as well as fast, automated variations of the experimental parameters. The parameters are directly measurable, which simplifies the documentation of extensive experiments.

The setup allows for the investigation of different parameter combinations like vocal fold elongation and adduction scenarios. Not only symmetric but also asymmetric vocal fold adduction levels can be adjusted, which was already presented in Ref. 40. Therewith, a simulation of voice disorders is possible, including muscle tension dysphonia by inducing asymmetric vocal fold adduction[13,16,18,20] and unilateral vocal fold paralysis by inducing adduction in only one vocal fold.[51,52]

Phonation onset and offset pressure and flow as a function of vocal fold adduction and elongation can be investigated in detail.

The setup is based on a simplified arytenoid cartilage motion that simulates a lateral cricoarytenoid muscle contraction leading to a rotation of the cartilage. More complex vocal fold adduction taking in account not only rotation, but also the sliding and tilting motion of the arytenoid cartilages will be done in future work.

The automated onset detection uses a threshold amplitude determined by the experimenter and is therewith based on a subjective assessment. In future, an automated threshold determination can be implemented with a fixed percentage of amplitude in comparison to the residual noise. This was used as indicator for phonation onset by Jiang *et al.*[9] using the acoustic signal.

Further improvement of the setup is planed but is always a compromise between a high complexity of parameter variation and the error rate and rapidity of the control circuit. Finally, further automatization of the system is limited by the large inter-subject variability of *ex vivo* larynges.

ACKNOWLEDGMENTS

This research was supported by Deutsche Forschungsgemeinschaft Grant No. DO1247/6-1. D.A.B.'s effort on this project was supported by National Institutes of

Health/National Institute on Deafness and Other Communication Disorders (NIH/NIDCD) Grant No. R01 DC013323.

[1]I. R. Titze, "The physics of small-amplitude oscillation of the vocal folds," J. Acoust. Soc. Am. **83**, 1536–1552 (1988).
[2]C. Storck, P. Juergens, C. Fischer, O. Haenni, F. Ebner, M. Wolfensberger, E. Sorantin, G. Friedrich, and M. Gugatschka, "Three-dimensional imaging of the larynx for pre-operative planning of laryngeal framework surgery," Eur. Arch. Otorhinolaryngol. **267**, 557–563 (2010).
[3]C. A. Rosen and C. B. Simpson, "Clinical evaluation of laryngeal disorders," in *Operative Techniques in Laryngology* (Springer, Berlin, 2008), Chaps. 1–7, pp. 3–48.
[4]D. K. Chhetri, J. Neubauer, and D. A. Berry, "Graded activation of the intrinsic laryngeal muscles for vocal fold posturing," J. Acoust. Soc. Am. **127**, 127–133 (2010).
[5]F. Alipour and R. C. Scherer, "On pressure-frequency relations in the excised larynx," J. Acoust. Soc. Am. **122**, 2296–2305 (2007).
[6]F. Alipour and S. Jaiswal, "Glottal airflow resistance in excised pig, sheep, and cow larynges," J. Voice **23**, 40–50 (2009).
[7]F. Alipour and S. Jaiswal, "Phonatory characteristics of excised pig, sheep, and cow larynges," J. Acoust. Soc. Am. **123**, 4572–4581 (2008).
[8]K. Inagi, N. P. Connor, T. Suzuki, C. N. Ford, D. M. Bless, and M. Nakajima, "Glottal configuration, acoustic, and aerodynamic changes induced by variation in suture direction in arytenoid adduction procedures," Ann. Otol. Rhinol. Laryngol. **111**, 861–870 (2002).
[9]J. J. Jiang, M. F. Regner, C. Tao, and S. Pauls, "Phonation threshold flow in elongated excised larynges," Ann. Otol. Rhinol. Laryngol. **117**, 548–553 (2008).
[10]M. F. Regner, C. Tao, P. Zhuang, and J. J. Jiang, "Onset and offset phonation threshold flow in excised canine larynges," Laryngoscope **118**, 1313–1317 (2008).
[11]E. Vilkman, "An apparatus for studying the role of the cricothyroid articulation in the voice production of excised human larynges," Folia Phoniatr. **39**, 169–177 (1987).
[12]Y. Zhang, W. J. Reynders, J. J. Jiang, and I. Tateya, "Determination of phonation instability pressure and phonation pressure range in excised larynges," J. Speech Lang. Hear. Res. **50**, 611–620 (2007).
[13]D. A. Berry, H. Herzel, I. R. Titze, and B. H. Story, "Bifurcations in excised larynx experiments," J. Voice **10**, 129–138 (1996).
[14]F. Alipour, E. M. Finnegan, and S. Jaiswal, "Phonatory characteristics of the excised human larynx in comparison to other species," J. Voice **27**, 441–447 (2013).
[15]M. Döllinger, J. Kobler, D. A. Berry, D. D. Mehta, G. Luegmair, and C. Bohr, "Experiments on analysing voice production: Excised (human, animal) and *in vivo* (animal) approaches," Curr. Bioinform. **6**, 286–304 (2011).
[16]M. R. Hoffman, K. Surender, E. E. Devine, and J. J. Jiang, "Classification of glottic insufficiency and tension asymmetry using a multilayer perceptron," Laryngoscope **122**, 2773–2780 (2012).
[17]G. Luegmair, "3D reconstruction of vocal fold surface dynamics in functional dysphonia," Ph.D. dissertation, Abt. für Phoniatrie and Pädaudiologie and der Hals-Nasen-Ohren Klinik, Erlangen, 2013.
[18]E. E. Devine, E. E. Bulleit, M. R. Hoffman, T. M. McCulloch, and J. J. Jiang, "Aerodynamic and nonlinear dynamic acoustic analysis of tension asymmetry in excised canine larynges," J. Speech Lang. Hear. Res. **55**, 1850–1861 (2012).
[19]A. Giovanni, M. Ouaknine, B. Guelfucci, P. Yu, M. Zanaret, and J. Triglia, "Nonlinear behavior of vocal fold vibration: The role of coupling between the vocal folds," J. Voice **13**, 465–476 (1999).
[20]R. Maunsell, M. Ouaknine, A. Giovanni, and A. Crespo, "Vibratory pattern of vocal folds under tension asymmetry," Otolaryngol. Head Neck Surg. **135**, 438–444 (2006).
[21]J. J. Jiang, K. Verdolini, N. Jennie, B. Aquino, and D. Hanson, "Effects of dehydration on phonation in excised canine larynges," Ann. Otol. Rhinol. Laryngol. **109**, 568–575 (2000).
[22]L. W. Plexico, M. J. Sandage, and K. Y. Faver, "Assessment of phonation threshold pressure: A critical review and clinical implications," Am. J. Speech Lang. Pathol. **20**, 348–366 (2011).
[23]D. G. Hottinger, C. Tao, and J. J. Jiang, "Comparing phonation threshold flow and pressure by abducting excised larynges," Laryngoscope **117**, 1695–1699 (2007).
[24]O. Köster, B. Marx, P. Gemmar, M. M. Hess, and H. J. Künzel, "Qualitative and quantitative analysis of voice onset by means of a multidimensional voice analysis system (MVAS) using high-speed imaging," J. Voice **13**, 355–374 (1999).
[25]M. F. Regner and J. J. Jiang, "Phonation threshold power in *ex vivo* laryngeal models," J. Voice **25**, 519–525 (2011).
[26]C. Tao, M. F. Regner, Y. Zhang, and J. J. Jiang, "Experimental and theoretical investigations of phonation threshold pressure as a function of vocal fold elongation," Acta Acust. Acust. **97**, 669–677 (2011).
[27]A. H. Mendelsohn and Z. Zhang, "Phonation threshold pressure and onset frequency in a two-layer physical model of the vocal folds," J. Acoust. Soc. Am. **130**, 2961–2968 (2011).
[28]D. K. Chhetri, J. Neubauer, and D. A. Berry, "Neuromuscular control of fundamental frequency and glottal posture at phonation onset," J. Acoust. Soc. Am. **131**, 1401–1412 (2012).
[29]R. L. Plant, G. L. Freed, and R. E. Plant, "Direct measurement of onset and offset phonation threshold pressure in normal subjects," J. Acoust. Soc. Am. **116**, 3640–3646 (2004).
[30]B. L. Smith, S. P. Nemcek, K. A. Swinarski, and J. J. Jiang, "Nonlinear source-filter coupling due to the addition of a simplified vocal tract model for excised larynx experiments," J. Voice **27**, 261–266 (2013).
[31]I. R. Titze, S. S. Schmidt, and M. R. Titze, "Phonation threshold pressure in a physical model of the vocal fold mucosa," J. Acoust. Soc. Am. **97**, 3080–3084 (1995).
[32]T. L. Shiba and D. K. Chhetri, "Dynamics of phonatory posturing at phonation onset," Laryngoscope **126**, 1837–1843 (2015).
[33]T. Mau, J. Muhlestein, S. Callahan, K. T. Weinheimer, and R. W. Chan, "Phonation threshold pressure and flow in excised human larynges," Laryngoscope **121**, 1743–1751 (2011).
[34]C. Lin and H. Wang, "Automatic estimation of voice onset time for word-initial stops by applying random forest to onset detection," J. Acoust. Soc. Am. **130**, 514–525 (2011).
[35]R. F. Orlikoff, D. D. Deliyski, R. J. Baken, and B. C. Watson, "Validation of a glottographic measure of vocal attack," J. Voice **23**, 164–168 (2009).
[36]M. Kunduk, Y. Yan, A. J. McWhorter, and D. Bless, "Investigation of voice initiation and voice offset characteristics with high-speed digital imaging," Logoped. Phoniatr. Vocol. **31**, 139–144 (2006).
[37]S. Petermann, S. Kniesburges, A. Ziethe, A. Schützenberger, and M. Döllinger, "Evaluation of analytical modeling functions for the phonation onset process," Comput. Math. Methods Med. **2016**, 1–10 (2016).
[38]T. Braunschweig, J. Flaschka, P. Schelhorn-Neise, and M. Döllinger, "High-speed video analysis of the phonation onset, with an application to the diagnosis of functional dysphonias," Med. Eng. Phys. **30**, 59–66 (2008).
[39]J. L. Kasperbauer, "A biomechanical study of the human cricoarytenoid joint," Laryngoscope **108**, 1704–1711 (1998).
[40]G. Luegmair, D. D. Mehta, J. B. Kobler, and M. Döllinger, "Three-dimensional optical reconstruction of vocal fold kinematics using high-speed video with a laser projection system," IEEE Trans. Med. Imag. **34**, 2572–2582 (2015).
[41]V. Birk, A. Sutor, M. Döllinger, C. Bohr, and S. Kniesburges, "Acoustic impact of ventricular folds on phonation studied in *ex vivo* human larynx models," Acta Acust. Acust. **102**, 244–256 (2016).
[42]R. W. Chan and I. R. Titze, "Effect of postmortem changes and freezing on the viscoelastic properties of vocal fold tissues," Ann. Biomed. Eng. **31**, 482–491 (2003).
[43]F. Alipour, S. Jaiswal, and E. S. Finnegan, "Aerodynamic and acoustic effects of false vocal folds and epiglottis in excised larynx models," Ann. Otol. Rhinol. Laryngol. **116**, 135–144 (2007).
[44]D. K. Chhetri, J. Neubauer, E. Sofer, and D. A. Berry, "Influence and interactions of laryngeal adductors and cricothyroid muscles on fundamental frequency and glottal posture control," J. Acoust. Soc. Am. **135**, 2052–2064 (2014).
[45]T. Y. Hsiao, C. M. Liu, E. S. Luschei, and I. R. Titze, "The effect of cricothyroid muscle action on the relation between subglottal pressure and fundamental frequency in an *in vivo* canine model," J. Voice **15**, 187–193 (2001).
[46]Jw. van den Berg, J. T. Zantema, and P. Doornenbal, "On the air resistance and the Bernoulli effect of the human larynx," J. Acoust. Soc. Am. **29**, 626–631 (1957).
[47]M. Döllinger, D. A. Berry, and S. Kniesburges, "Dynamic vocal fold parameters with changing adduction in *ex-vivo* hemilarynx experiments," J. Acoust. Soc. Am. **139**, 2372–2385 (2016).

[48]I. R. Titze, "On the relation between subglottal pressure and fundamental frequency in phonation," J. Acoust. Soc. Am. **85**, 901–906 (1989).
[49]J. Lohscheller, U. Eysholdt, H. Toy, and M. Döllinger, "Phonovibrography: Mapping high-speed movies of vocal fold vibrations into 2-D diagrams for visualizing and analyzing the underlying laryngeal dynamics," IEEE Trans. Med. Imag. **27**, 300–309 (2008).
[50]R. E. Witt, M. F. Regner, C. Tao, A. L. Rieves, P. Zhuang, and J. J. Jiang, "Effect of dehydration on phonation threshold flow in excised canine larynges," Ann. Otol. Rhinol. Laryngol. **118**, 154–159 (2009).
[51]L. Czerwonka, C. N. Ford, A. T. Machi, G. E. Leverson, and J. J. Jiang, "A-P positioning of medialization thyroplasty in an excised larynx model," Laryngoscope **119**, 591–596 (2009).
[52]T. M. McCulloch, M. R. Hoffman, K. E. McAvoy, and J. J. Jiang, "Initial investigation of anterior approach to arytenoid adduction in excised larynges," Laryngoscope **123**, 942–947 (2013).